Journal of Electroceramics 1:1, 41–49, 1997

Simplified Analytical Treatment of Defect Equilibria: Applications to Oxides with Multivalent Dopants

OFER PORAT & HARRY L. TULLER

Crystal Physics and Electroceramics Laboratory, Department of Materials Science and Engineering, Massachusetts Institute of Technology, Cambridge, MA 02139, USA

Received October 22, 1996; Accepted December 5, 1996

Abstract. A simplified analytical treatment of rather complex defect equilibria involving systems with multivalent dopants is presented. This approach is first demonstrated for the case of $Gd_2Ti_2O_7$ doped with multiple valent donors, in which the effects of variations in donor ionization levels and in the equilibrium constants on the defect equilibria are examined. The conductivity data of U doped CeO_2 are then evaluated, leading to equilibrium constants in good agreement with previous results, but allowing a more complete analysis.

Keywords: defect equilibria, multivalent dopants, analytical treatment, pyrochlores

Introduction

The growing interest in the development of solid oxide fuel cells, oxygen sensors and oxygen exchange membranes [1] has generated increased demands for higher oxygen ion conductivities in solid oxide electrolyte materials, and high but controlled levels of mixed ionic-electronic conduction (MIEC) in electrode or oxygen exchange membrane materials.

In recent reports [2], we have emphasized the need for versatile host oxides in which the levels of ionic and electronic conductivities can be controlled in such a way that structurally and chemically compatible solid electrolytes and MIECs can be derived. Such compatible systems enable ease of fabrication and extended life [3]. We have found that the pyrochlore oxide system, $Gd_2(Ti_xZr_{1-x})_2O_7$ (GTZ) exhibits the level of versatility required for the above objectives. GTZ with $x \leq 0.3$ is intrinsically disordered and exhibits high levels of predominantly oxygen ion conductivity [4]. The titanate end-member, GT ($x = 0$), is also an excellent ionic conductor when doped with Ca on the Gd site [5].

In the process of attempting to simultaneously introduce high levels of ionic and electronic conductivity into GT, we have found it useful to dope the materials with multivalent ions such as Mn [6], Mo [7] and Ru [8]. This, however, has resulted in systems which are much more difficult to analyze. First, the multiple oxidation states of the dopants considerably complicate the defect structure. Second, because these elements often form impurity bands, the number of possible mobile electronic species increases. We found that the standard use of the Brouwer approximation [9] was inadequate in treating key experimental data which often fell within transition regimes separating the approximate Brouwer regimes.

Re-examining the approaches used for solving the defect relations, we successfully developed an analytical solution considerably more convenient then the numerical solutions often used [10]. In this paper we describe the approach taken to achieve such analytical solutions even under circumstances where such solutions were believed not to exist [9,10]. This approach was first applied, in a simplified manner, by Porat and Riess [11,12], followed more recently by a more general approach by Spinolo and Anselmi-Tamburini [13]. We illustrate the utility of these solutions by applying them to a number of relevant problems of interest.

In a following paper [14], we examine how impurity band contributions to the total electrical

conductivity can be predicted on the basis of the analytical solution to the defect density obtained in this paper, the degree of impurity band filling and the proposed electronic carrier mobility mechanisms (small versus large polaron) in the various bands.

In subsequent papers, we apply the combined defect and mobility analyses to experimental measurements recently obtained on GT doped with Mn, Nb, W or Mo. Preliminary experimental results on these systems may be found in references [6,7,15], respectively.

Defect Chemistry

In many oxide systems lattice disorder occurs predominantly on the anion sublattice. Under these circumstances, the intrinsic lattice defects are anion Frenkel pairs, i.e., doubly ionized oxygen interstitials and vacancies, O_i'' and $V_O^{\bullet\bullet}$, respectively, while the cations, represented as M, are immobile. At times, one can find these defects in a lower ionization state—i.e., singly ionized O_i' and $V_O^{\bullet}$. The charged oxygen defects may also be compensated by electronic carriers, i.e. electrons e′, and holes, $h^{\bullet}$, or by charged impurities such as acceptors: A_M' and A_M'' and donors: $D_M^{\bullet}$ and $D_M^{\bullet\bullet}$. The impurities may be deep or shallow, neutral, singly or multi-ionized (here we treat a maximum of two ionization states). The neutrality condition, under these circumstances, is written as:

$$[O_i'] + 2[O_i''] + [A_M'] + 2[A_M''] + n = [V_O^{\bullet}] + 2[V_O^{\bullet\bullet}] + [D_M^{\bullet}] + 2[D_M^{\bullet\bullet}] + p \quad (1)$$

[ ] stands for ionic defect concentration, n and p are the concentration of electrons and holes in the conduction and valence bands, respectively. For the purpose of demonstrating our approach to solving such a complex equilibrium condition analytically, we assume a donor doped system, i.e.:

$$[O_i'] + 2[O_i''] + n = [V_O^{\bullet}] + 2[V_O^{\bullet\bullet}] + [D_M^{\bullet}] + 2[D_M^{\bullet\bullet}] + p \quad (1a)$$

The same treatment can be performed readily for the complete defect system, i.e., Eq. (1), as will become obvious from the following.

The relevant defect formation reactions (ignoring neutral oxygen defects), along with their mass action relations, assuming dilute solution, are:
Reduction reaction:

$$O_O \Leftrightarrow \frac{1}{2}O_2 + V_O^{\bullet\bullet} + 2e',\ K_R(T) = \mathrm{Po}_2^{1/2}[V_O^{\bullet\bullet}]n^2 \quad (2)$$

Frenkel reaction:

$$O_O \Leftrightarrow V_O^{\bullet\bullet} + O_i'',\ K_F(T) = [V_O^{\bullet\bullet}][O_i''] \quad (3)$$

Ionization reactions:

$$V_O^{\bullet} \Leftrightarrow V_O^{\bullet\bullet} + e',\ K_{V2}(T)[V_O^{\bullet}] = [V_O^{\bullet\bullet}]n \quad (4)$$

$$O_i'' \Leftrightarrow O_i' + e',\ K_{I2}(T)[O_i''] = [O_i']n \quad (5)$$

$$D_M^x \Leftrightarrow D_M^{\bullet} + e',\ K_{D1}(T)[D_M^x] = [D_M^{\bullet}]n \quad (6)$$

$$D_M^{\bullet} \Leftrightarrow D_M^{\bullet\bullet} + e',\ K_{D2}(T)[D_M^{\bullet}] = [D_M^{\bullet\bullet}]n \quad (7)$$

Electron-hole generation-recombination:

$$\mathrm{nil} \Leftrightarrow e' + h^{\bullet},\ K_e = n \cdot p \quad (8)$$

K_R, K_F, K_{V2}, K_{I2}, K_{D1}, K_{D2} and K_e are the reaction constants, having the form $K(T) = K_0 \exp(-E/k_BT)$, where K_0 includes the entropy term, E is the reaction enthalpy, and k_B is the Boltzmann constant.

In addition we have the law of mass conversation :

$$[D_M^x] + [D_M^{\bullet}] + [D_M^{\bullet\bullet}] = \text{constant} \equiv D \quad (9)$$

Eqs. (1)–(9) allow one to calculate the defect concentrations as a function of Po_2, T and D.

We first present all the defect concentrations as a function of n, using Eqs. (1)–(9):

$$[V_O^{\bullet\bullet}] = \frac{K_R}{n^2}\mathrm{Po}_2^{-1/2} \quad (10)$$

$$[O_i''] = \frac{K_F n^2}{K_R}\mathrm{Po}_2^{1/2} \quad (11)$$

$$[V_O^{\bullet}] = \frac{K_R}{K_{V2}n}\mathrm{Po}_2^{-1/2} \quad (12)$$

$$[O_i'] = \frac{K_{I2}K_F n}{K_R}\mathrm{Po}_2^{1/2} \quad (13)$$

$$[D_M^{\bullet}] = \frac{K_{D1}Dn}{n^2 + nK_{D1} + K_{D1}K_{D2}} \quad (14)$$

$$[D_M^{\bullet\bullet}] = \frac{K_{D1}K_{D2}D}{n^2 + nK_{D1} + K_{D1}K_{D2}} \quad (15)$$

$$[D_M^x] = \frac{Dn^2}{n^2 + nK_{D1} + K_{D1}K_{D2}} \quad (16)$$

$$p = K_e/n \quad (17)$$

By substituting Eqs. (10)–(17) into the neutrality equation (Eq. (1a)), one obtains a relation between n and Po_2 given by:

$$\begin{aligned} n &= [V_O^{\bullet}] + 2[V_O^{\bullet\bullet}] + [D_M^{\bullet}] + 2[D_M^{\bullet\bullet}] + p - [O_i'] - 2[O_i''] \\ &= \frac{K_R}{K_{V2}n}Po_2^{-1/2} + 2\frac{K_R}{n^2}Po_2^{-1/2} + \frac{K_{D1}Dn}{n^2 + nK_{D1} + K_{D1}K_{D2}} \\ &\quad + 2\frac{K_{D1}K_{D2}D}{n^2 + nK_{D1} + K_{D1}K_{D2}} + \frac{K_e}{n} - \frac{K_{12}K_F n}{K_R}Po_2^{1/2} \\ &\quad - 2\frac{K_F n^2}{K_R}Po_2^{1/2} \end{aligned} \tag{18}$$

If, as is commonly done, one attempts to solve Eq. (18) for n, one obtains a 6^{th} order polynomial in n, leading to an non-analytical solution [10]. One may note, however, that the Po_2 dependence comes only from the reduction reaction (2). By solving instead for $Po_2^{1/2}$, one obtains a simple quadratic equation with only one physically meaningful solution:

$$Po_2^{1/2}(n) = [-b + (b^2 - 4ac)^{1/2}]/2a \tag{19}$$

with:

$$\begin{aligned} a &= [K_{12}K_F n/K_R + 2K_F n^2/K_R] \\ b &= \left[n - \frac{K_{D1}Dn + 2K_{D1}K_{D2}D}{n^2 + nK_{D1} + K_{D1}K_{D2}} - \frac{K_e}{n}\right] \\ c &= [K_R/K_{V2}n + 2K_R/n^2] \end{aligned}$$

By substituting values for the equilibrium constants and appropriate test values for n into Eq. (18), one obtains corresponding values for Po_2 at each isotherm. These coupled values of n and Po_2 can then be substituted into Eqs. (10)–(17), to obtain values for the other defects of interest.

It is easily seen that the addition of the other defects contained in Eq. (1) will not change the quadratic nature in Po_2 of Eq. (18), and can be used to obtain an analytical solution for the complete case. The key principle is to present the defect concentration linearly in either $Po_2^{1/2}$ or $Po_2^{-1/2}$. This principle can be further generalized to systems in which divalent cation defects are also included in the neutrality equation.

Defect Concentrations in Donor Doped $Gd_2Ti_2O_7$

To illustrate the utility of the analytical solutions to the defect relations of the form presented in Eq. (18), we use the system $Gd_2Ti_2O_7$, for which many of the key equilibrium constants (see Table 1) have recently been reported [8,16]. In Fig. 1 we show the calculated defect concentrations as a function of Po_2 at 1000°C. In this case, we selected an imaginary donor with rather deep levels, $E_{D1} = 0.53$ eV and $E_{D2} = 2.78$ eV, where E_{D1} and E_{D2} are the locations of the first and second donor ionization levels, respectively, and a total donor concentration of 10% ($D = 1.5 \times 10^{21}$ cm^{-3}).

While the Po_2 dependences of the defect concentrations vary continuously in the transition regions, it remains useful, for purposes of comparison with conventional analysis, to examine the different Brouwer regions. Figure 1 can be divided into four different Brouwer regions. In each, one defect on either side of Eq. (1a) approximately controls the neutrality equation, and as a consequence, the Po_2 dependence of the various defects. At the highest Po_2 (region I), D is completely oxidized to $D_M^{\bullet}$, and is compensated by O_i'': $[D_M^{\bullet}] = 2[O_i'']$ (see Fig. 1). At lower Po_2 (region II), D is largely de-ionized ($[D_M^x] > [D_M^{\bullet}]$) but the reduced neutrality condition remains $[D_M^{\bullet}] = 2[O_i'']$. At even lower Po_2 (region III), the majority of donors remain un-ionized, nevertheless $D_M^{\bullet}$ and the compensating electrons, n, still represent the dominant charged species: $n = [D_M^{\bullet}]$. At the lowest Po_2, (region IV), the reduction of the host titanium takes over, leading to the neutrality condition $n = 2[V_O^{\bullet\bullet}]$. The Po_2 dependence of each defect is altered when moving from one Po_2 region to another. Note, that the prediction of the existence of region II would not be obvious taking the Brouwer approximation approach. Table 2 summarizes the various approximate neutrality relations and the corresponding defect $-Po_2$ dependences.

Table 1. Values of reaction constants of $Gd_2Ti_2O_7$ at 1000°C [8,16] used to prepare Fig. 1. K_{D1} and K_{D2} were selected for an imaginary donor impurity

K_F (cm^{-6})	K_R (cm^{-9} atm$^{1/2}$)	K_{V2} (cm^{-3})	K_{I2} (cm^{-3})	K_e (cm^{-6})	K_{D1} (cm^{-3})	K_{D2} (cm^{-3})
10^{33}	1.5×10^{47}	10^{25}	10^{12}	4×10^{31}	10^{17}	10^{10}

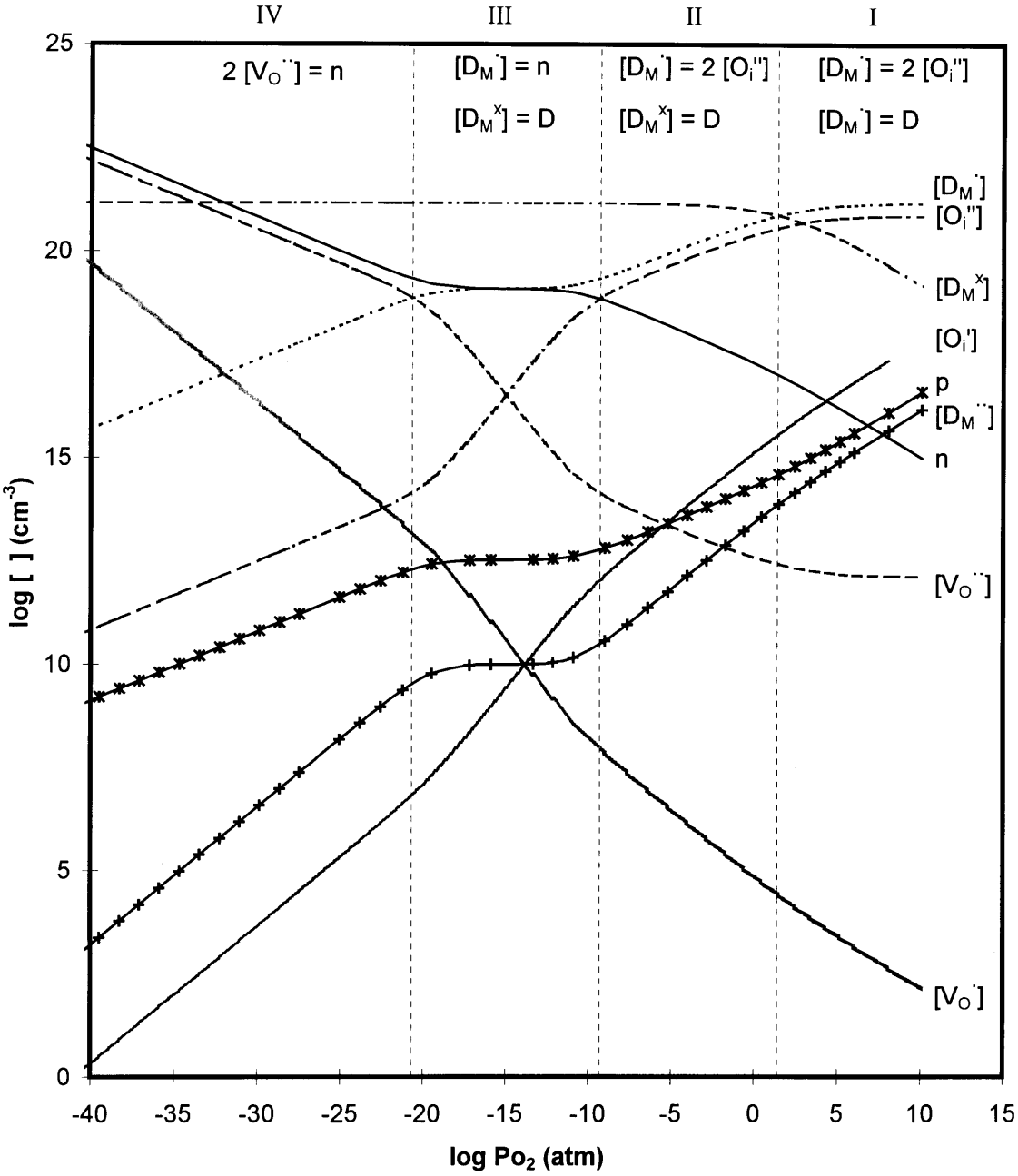

Fig. 1. Model prediction of the atmospheric dependence of defect concentrations in donor doped $Gd_2Ti_2O_7$. Roman numerals represent the different approximate electroneutrality conditions (see text). Vertical dashed lines represent region boundaries.

Impact of Donor Ionization Energies on the Defect Equilibria

As might be expected, the defect concentrations and their Po_2 sensitivities are strongly dependent on the choice of the donor dopants. This is illustrated in Fig. 2, in which we plot n for five different cases. Again we use the constants from Table 1 and $D = 10$ mol%. We consider the following cases: (#1) The two donor states are shallow (i.e., in region III $n = 2D$). (#2) The first ionization state is shallow, while the second is very deep. (#3) The two states are

Table 2. The slope $\partial\log[\ ]/\partial\log Po_2$ of the various defects at the different Po_2 regions (EC: electroneutrality condition)

EC	$2[O_i'']=[D_M^{\bullet}]$		$n=[D_M^{\bullet}]$	$n=[V_O^{\bullet\bullet}]$
Region →	I	II	III	IV
Defect ↓	$[D_M^x]\ll D$	$[D_M^x]\sim D$		
n	−1/4	−1/6	0	−1/6
p	1/4	1/6	0	1/6
$V_O^{\bullet\bullet}$	0	−1/6	−1/2	−1/6
O_i''	0	1/6	1/2	1/6
$V_O^{\bullet}$	−1/4	−1/3	−1/2	−1/3
O_i'	1/4	1/3	1/2	1/3
D_M^x	−1/4	0	0	0
$D_M^{\bullet}$	0	1/6	0	1/6
$D_M^{\bullet\bullet}$	1/4	1/3	0	1/3

rather deep, and are close in energy. (#4) The first state is rather deep, while the second is much deeper. (#5) Both levels are very deep, with virtually no ionization. The Po_2 dependence of the other defects can be derived from n using Eqs. (10)–(17).

Due to the shallow ionization energies corresponding to curves #1 and #2, complete ionization of at least one level results in $n\approx D$ in regime III. These curves show three regions instead of four, since region II is largely non-existant, and this presents, for n, a single slope of $-1/4$ at high Po_2. Note the marginal difference between the two curves, only a factor of 2 in the plateau region (III).

For the other extreme case of very deep donors (curve #5). the condition $n=2[V_O^{\bullet\bullet}]$, regime IV, extends to much higher Po_2. Here, at intermediate Po_2, Frenkel pairs dominate, $[V_O^{\bullet\bullet}]=[O_i'']$, rather than donors, and $n\propto Po_2^{-1/4}$. At the highest Po_2 we have $p=2[O_i'']$ and as a consequence $n\propto Po_2^{-1/6}$.

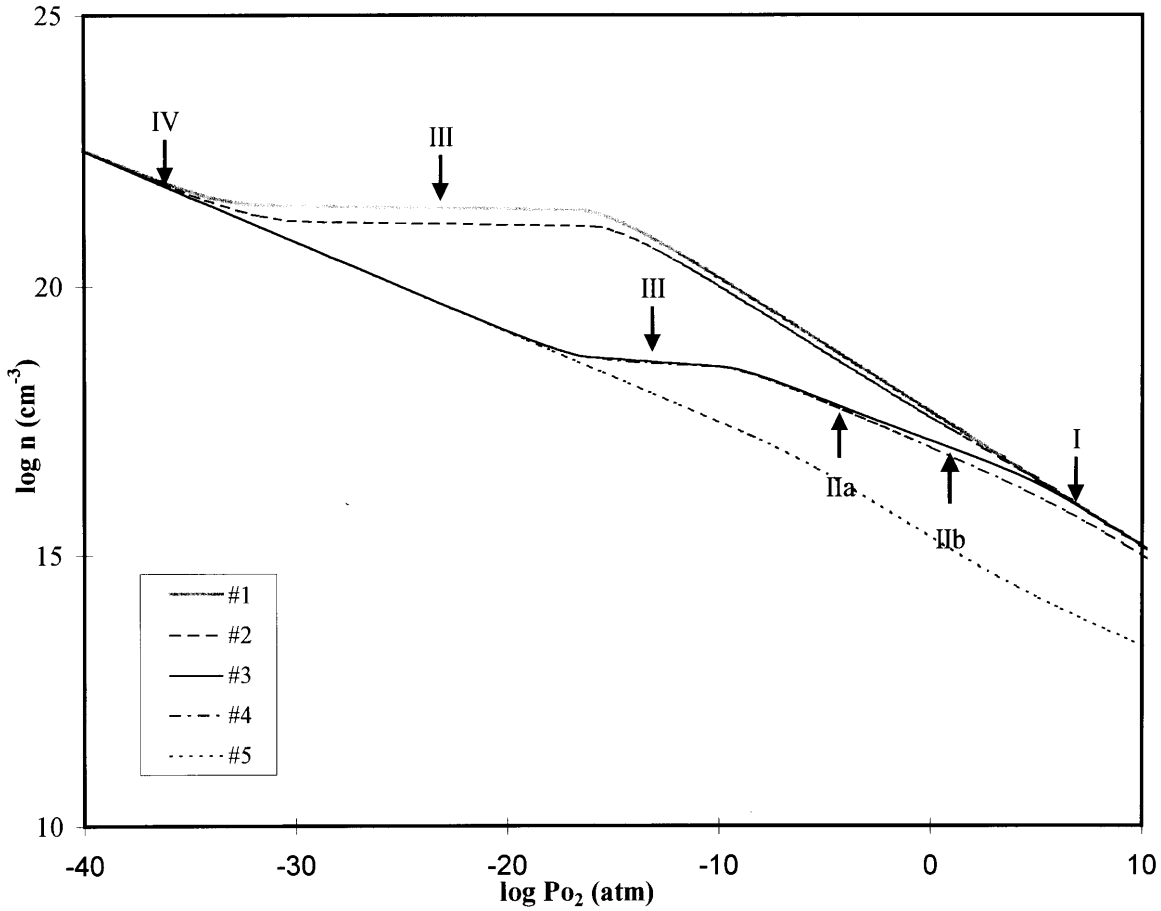

Fig. 2. Po_2 dependence of n for different dopant energies: #1: Two shallow donor levels. #2: One shallow donor level. #3: Two deep but close levels. #4: One deep and a second very deep level. #5: Undoped system. Roman numerals represent the different electroneutrality conditions as in Fig. 1.

The two curves representing reasonably deep levels (#3, #4), exhibit similar behavior at low and intermediate Po_2's-regions IV and III respectively. Note that region III shrinks, as compared to that in curves #1 and #2. At higher Po_2, curve #4 exhibits the same Po_2 dependence as in Fig. 1, i.e., $n \propto Po_2^{-1/6}$ in region II, while $n \propto Po_2^{-1/4}$ in region I. Curve #3 shows an interesting behavior, and is composed of three different regions at high Po_2. This is due to the fact that at this Po_2 range the neutrality condition becomes $2[O_i''] = [D_M^{\bullet}] + 2[D_M^{\bullet\bullet}]$. Increasing Po_2 and moving down from the plateau (region III), oxidizes D_M^x to $D_M^{\bullet}$, therefore $2[O_i''] = [D_M^{\bullet}]$ and again $n \propto Po_2^{-1/6}$ (region IIa). Then, the second ionization takes over so $[O_i''] = 2[D_M^{\bullet}]$ and $n \propto Po_2^{-1/8}$ (IIb). This defect regime was not found for the parameters used to calculate Fig. 1. Lastly D_M^x is completely ionized at sufficient high Po_2 (region I), and $n \propto Po_2^{-1/4}$.

Impact of Reaction Constants of Host Material on Defect Equilibria

Next we demonstrate how changes in the magnitude of the different equilibrium constants, K_R, K_F, K_{I2} and K_{V2} impact defect densities and the location of the different defect regimes. These constants, for example, are altered as one varies the composition of a solid solution. For example, increasing x in $Gd_2(Zr_xTi_{1-x})_2O_7$ leads to large and systematic increases in Frenkel disorder and the corresponding Frenkel constant [17]. The effects of such variations on n are illustrated in Fig. 3. Curve #1 is calculated with the same equilibrium constants as used before in

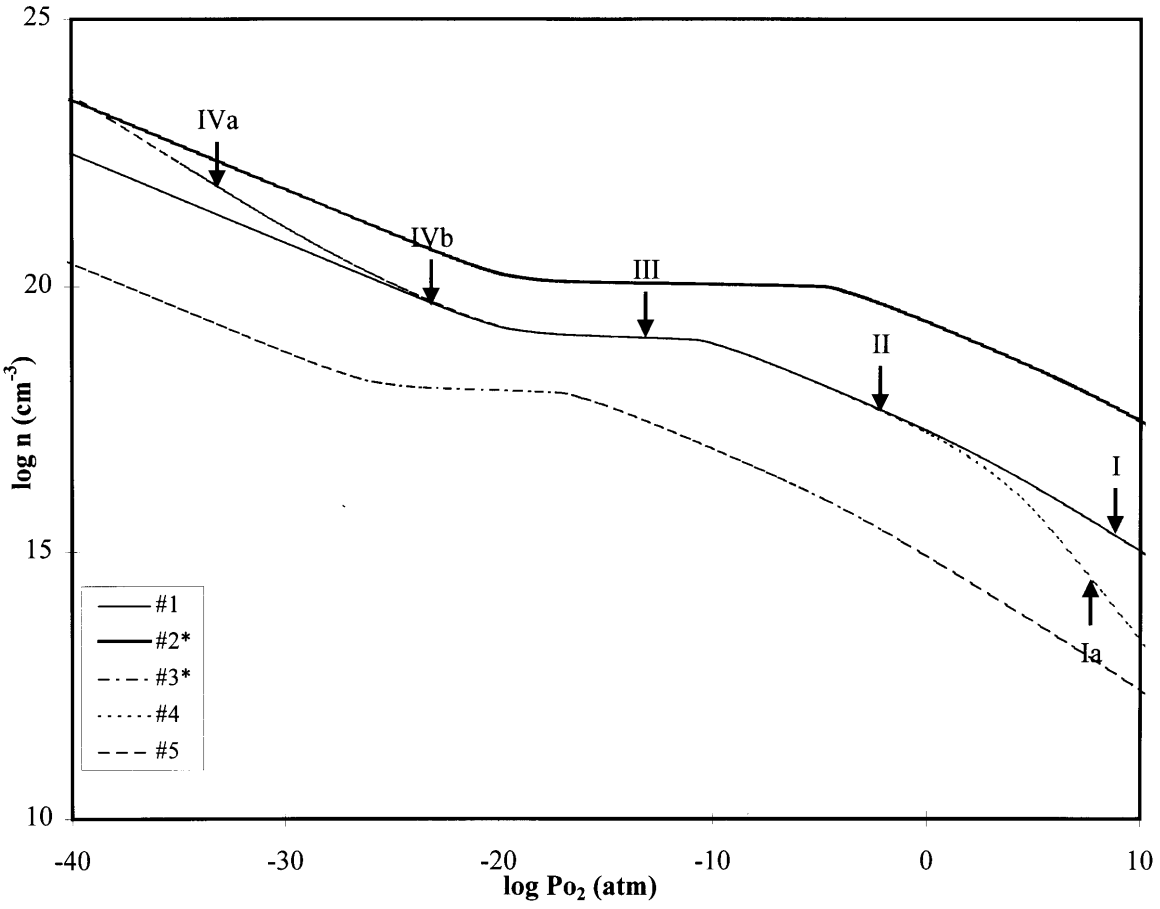

Fig 3. Po_2 dependence of n for different equilibrium constants of the host material. #1: reference curve, as in Fig. 1 #2: smaller K_F #3: smaller K_R #4: larger K_{I2} and #5: smaller K_{V2}, respectively, compared to the corresponding values in #1. Roman numerals as in Fig. 1. *The calculated data for curves #2 and #3 are offset by factors of 10 and 0.1, respectively, for clarity.

Fig. 1, and serves as a reference. When one decreases K_F by three orders of magnitude (curve #2), regime III broadens by extending to higher Po's. This follows from the fact that the intrinsic value of $[O_i'']$ is smaller, and so the condition $2[O_i''] = [D_M^{\bullet}]$ is only achieved at higher Po_2.

Curve #3 was calculated using a smaller reduction constant K_R $(1 \times 10^{44}\,\mathrm{cm}^{-3})$. This results in an extension of region III to lower Po_2's, since now lower Po_2's are required to generate $[V_O^{\bullet\bullet}]$ equal to the same $[D_M^{\bullet}]$. On the other hand, the II/III boundary shifts to lower Po_2 since a less oxidizing environment is necessary to generate sufficient numbers of interstitials to satisfy $2[O_i''] = [D_M^{\bullet}]$.

Curve #4 was calculated using a larger K_{I2} constant (by a factor of 10^4), i.e., an increased concentration of singly ionized oxygen interstitials, O_i'. This reaction, which is enhanced at lower temperatures and higher Po_2's, results in an interesting trend at high Po_2. Since the neutrality condition at high Po_2's becomes $[D_M^{\bullet}] = 2[O_i''] + [O_i']$, with O_i'' more important at intermediate Po_2 and more important at higher Po_2, the slope of log(n) vs log(Po_2) changes from $-1/6$ in region II to $-1/2$ in region Ia.

In a similar manner, curve #5 was calculated with a 10^5 times smaller value for K_{V2}. This results in a separate region (IVa), where the neutrality condition is $n = [V_O^{\bullet}]$, resulting in a change of slope for n at the lowest Po_2's from $-1/6$ in region IVb to $-1/4$ in region IVa.

Electrical Conductivity in Uranium Doped CeO_2

To further test the utility of this solution, we apply it to our earlier measurements of the electrical

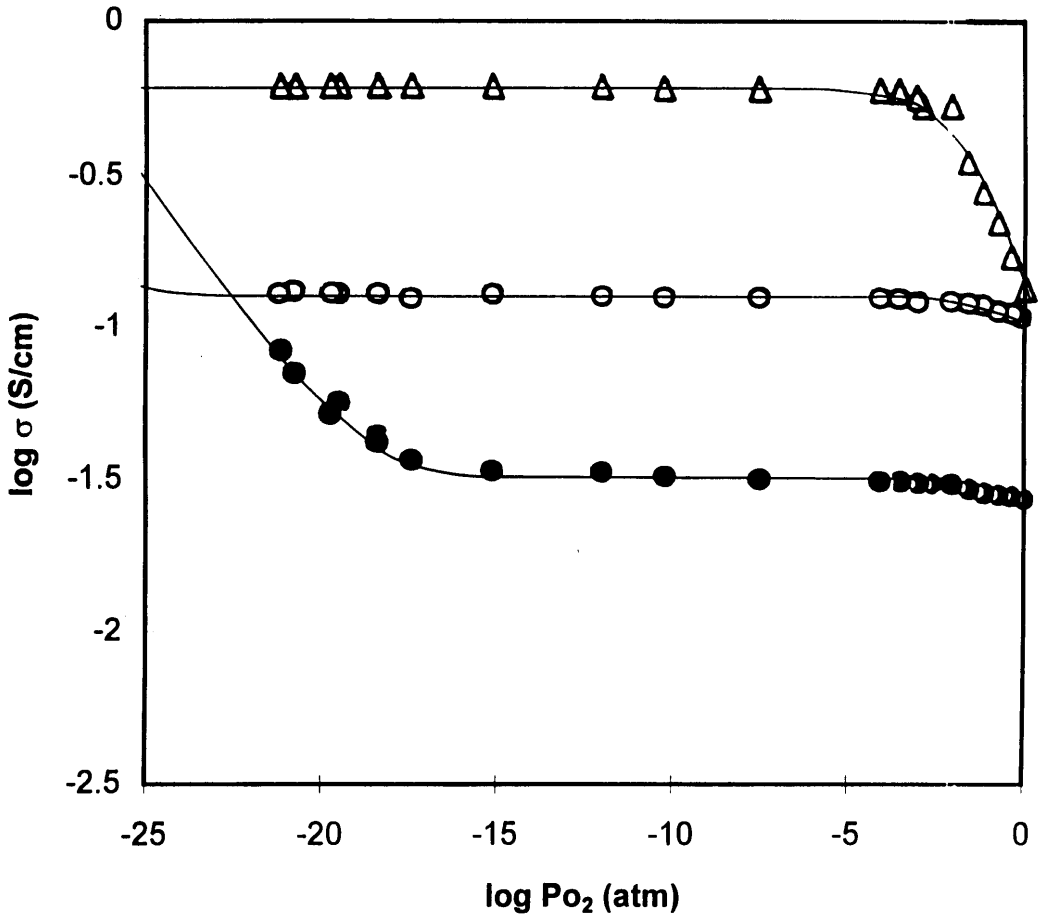

Fig. 4. Solid lines correspond to fit of model to experimental electrical conductivity data of: $Ce_{0.95}U_{0.05}O_2$ (●), $Ce_{0.99}U_{0.01}O_2$ (○) and $Ce_{0.999}U_{0.001}O_2$ (△) at 666°C. Experimental data from [18].

Table 3. Values of equilibrium constants for uranium doped CeO_2 at 666°C

	Present study			Stratton and Tuller [18]	
Composition	K_F (cm^{-6})	K_R (cm^{-9} $atm^{1/2}$)	K_{I2} (cm^{-3})	K_F (cm^{-6})	K_R (cm^{-9} $atm^{1/2}$)
$Ce_{0.999}U_{0.001}O_2$	9×10^{27}	4×10^{48}		5.8×10^{27}	2.25×10^{48}
$Ce_{0.99}U_{0.01}O_2$	1.5×10^{26}	4×10^{47}		1.45×10^{26}	4.1×10^{47}
$Ce_{0.95}U_{0.05}O_2$	10×10^{25}	1.75×10^{47}	5×10^{21}	9.7×10^{25}	1.75×10^{47}

conductivity of uranium doped ceria [18]. While the key elements of the defect equilibria of this system were determined using a more approximate approach, some details of the dependence of σ on Po_2 were not refined. As before, we assume predominant *n*-type conductivity, $\sigma_e = en\mu_e$, where e is the elementary charge and μ_e is the electron mobility. Figure 4 presents the results of fitting Eq. (19) to the experimental data reported for $Ce_{1-x}U_xO_2$ with $x = 0.001$, 0.01 and 0.05 at 666°C [18], with μ_e taken from the same reference. In Table 3 we present values for K_R, K_F obtained from this fitting, as compared to literature values. While our results are in good agreement with previous results, we also successfully fit the reaction constant K_{I2} of Eq. (5), by careful analysis of the Po_2 dependence of σ_e at high Po_2 for $Ce_{0.95}U_{0.05}O_2$.

Summary

We have presented an improved means of calculating defect concentrations in systems with donors and/or acceptors with multiple valence. By rearrangement of the neutrality equation, one obtains Po_2 as a function of n instead of $n(Po_2)$. This enables a simple analytical solution, even in a system with many defect types.

This principle is demonstrated for the case of doped $Gd_2Ti_2O_7$ with multiple valent donors, in which the effect of variation in donor ionization levels and in the equilibrium constants on defect concentrations and their respective Po_2 dependences are examined. New, unexpected defect regimes are identified in this manner.

The model was fit to conductivity data previously reported for uranium doped ceria. The equilibrium constants derived in this manner were found to be in good agreement with previous results. The present, more sophisticated model allowed, however, for the first time, extraction of values of K_{I2}.

Acknowledgment

This work was supported by Basic Energy Sciences, Department of Energy under Grant #DE-FGO2-86ER45261. The Authors thank Dr. T. Norby for bringing [13] to the attention of the authors during the review process.

References

1. M.C. Williams, pp. 10–19 in *Solid Oxide Fuel Cells IV*, M. Dokia, O. Yamamoto, T. Tagawa, and S.C. Singhal, eds. (The Electrochemical Society, Pennington, NJ, 1995).
2. H.L. Tuller, pp. 139–153 in *High Temperature Electrochemistry: Ceramics and Metals* F.W. Poulsen, N. Bonanos, S. Linderoth, M. Mogensen, and B. Zachau-Christiansen, eds. (Risø National Laboratory, Roskilde, Denmark, 1996).
3. H.L. Tuller, S.A. Kramer, and M.A. Spears, US Patent (#5,403,461, April 4, 1995).
4. H.L. Tuller, S.A. Kramer, and M.A. Spears, pp. 151–173 in *High Temperature Electrochemical Behavior of Fast Ion and Mixed Conductors* F.W. Poulsen, J.J. Bentzen, T. Jakobsen, E. Skou, and M.J.L. Ostergaard, eds. (Risø National Laboratory, Roskilde, Denmark, 1993).
5. S. Kramer and H.L. Tuller, *Solid State Ionics*, **82**, 15–23 (1995).
6. O. Porat, M.A. Spears, C. Heremans, I. Kosacki, and H.L. Tuller, *Solid State Ionics*, **86–88**, 285–288 (1996).
7. O. Porat, C. Heremans, and H.L. Tuller, *J. Am. Ceram. Soc.* (in press).
8. M.A. Spears and H.L. Tuller, pp. 94–105 in *Ionic and Mixed conducting Ceramics*, (Proc. Vol. 94-12). T.A. Ramanarayanan, W.L. Worrell, and H.L. Tuller, eds. (The Electrochemical Society, Pennington, NJ, 1994).
9. G. Brouwer, *Philips Research Repts.*, **9**, 366 (1954).
10. M.A. Spears and H.L. Tuller, pp. 271–288 in *Solid State Ionics IV (vol. 369),* G.A. Nazri, J.-M. Tarascon, and M. Schreiber, eds. (Materials Research Society, Pittsburgh, PA, 1995).
11. O. Porat, Ph.D. Thesis, The Technion, Israel Institute of Technology (1994).
12. O. Porat and I. Riess, *Solid State Ionics*, **81**, 29 (1995).
13. G. Spinolo and U. Anselmi-Tamburini, Ber. Bunsenges. *Phys. Chem.*, **99**, 87–90 (1995).
14. O. Porat and H.L. Tuller, in preparation.
15. I. Kosacki and H.L. Tuller, pp. 703–708 in *Solid State Ionics IV, (vol. 369)*, G.A. Nazri, J.-M. Tarascon, and M. Schreiber, eds.

(Materials Research Society, Pittsburgh, PA, 1995).
16. M. Spears and H.L. Tuller, pp. 301–306 in *Solid State Ionics III (Vol. 293)*.G-A. Nazri, J-M. Tarascon, and M. Armand, eds. (Materials Research Society, Pittsburgh, PA, 1993).
17. P.K. Moon and H.L. Tuller, *Solid State Ionics*, **28–30**, 470–74 (1988).
18. T.G. Stratton and H.L. Tuller, *J. Chem. Soc., Faraday Trans.* 2, **83**, 1143–56 (1987).